Supplementary Information

In situ released bacterial membrane vesicles activate STING pathway via boosting intracellular DNA pool for immunotherapy

Wenjie Wang,[a,b] Anjun Song,[a,b] Fang Pu,[a,b] Yanjie Zhang,[a,b] Jinsong Ren,[a,b] and Xiaogang Qu*[a,b]*

Experimental Procedures

Materials

$Fe(acac)_3$ (98%), $Co(acac)_3$ (98%), $Ni(acac)_2$ (98%), oleylamine (OAM, 80-90%), Stearyl trimethyl aminium·bromide (STAB, 98%) N-hydroxysuccinimide (NHS), and N-(3-dimethylaminopropyl)-N'-ethylcabodiimide (EDC) hydrochloride were purchased from Innochem. $SnCl_2$ (98%), $PdCl_2$(98%), ascorbic acid (AA, 99%), octadecene (ODE, 90%), dopamine hydrochloride and FITC-PEG-SH were purchased from aladdin. 1,4-benzenedicarboximidamide (2·2Cl) and tetrakis(4-carboxylic acid phenyl) methane (TBA_4·4) were purchased from EXTENSION. All chemicals were used as received without further purification.

Characterization

Scanning electron microscope (SEM) images were recorded on a Hitachi S-4800 FESEM at a working voltage of 10 kV and working current of 10 A. Transmission electron microscope (TEM) images were obtained on a TECNAI G2 equipped with energy dispersive spectroscopic (EDS) at 200 kV. X-ray diffractometer (XRD) measurements were performed on Bruker D8 Advance using Cu Kα radiation. The content of metallic element was analyzed on the Inductively Coupled Plasma-Optical Emission Spectrometry (ICP-OES, X Series 2, Thermo Scientific, USA). The UV-Vis absorption spectra were recorded using a JASCO V550 UV-Visible spectrophotometer. The flow cytometry data were obtained by BD LSRFortessa™ Cell Analyzer. The ζ –potential of the nanoparticles was measured in a Zetasizer 3000HS analyzer. The bondcleavage reaction in cells was observed via a confocal laser scanning microscope (CLSM, Nikon Eclipse Ni-E, Japan).

Purification and characterization of OMVs.

Escherichia Coli was grown on liquid luria broth (LB) medium cultured in a rotary shaker at 37 °C for 6 h and then refreshed with LB medium at 1:100 dilutions. The shaking flask cultures were grown until the OD_{600} value of the medium reached approximately 1.0, indicating the logarithmic growth phase. OMVs were collected as follows. Briefly, 500 ml bacteria culture medium was centrifuged at 5,000g for 30 min to remove the bacteria, followed by filtering through a 0.45 μm polyethersulfone filter (Millipore). The filtrate was

then concentrated using centrifugal filters with a molecular weight cut-off of 100 kDa (Millipore). The concentrated medium was pelleted by ultracentrifugation at 150,000g for 3 h at 4 °C, then the pellet was suspended in sterile PBS and ultracentrifuged at 150,000g for 3 h at 4 °C. Finally, the pellet was resuspended in PBS as the stock OMV preparation and subjected to agar plating to ensure the lack of bacterial contamination. Dynamic light scattering (DLS) and transmission electron microscopy (TEM) were used to characterize the size and morphology of OMVs.

Synthesis of PtRhBiSnSb HEA nanoplates

In the typical synthesis of FeCoNiSnPd nanoplates, 14 mg $Fe(acac)_3$, 14 mg $Co(acac)_3$, 10 mg $Ni(acac)_2$, 9 mg $SnCl_2$, 7 mg $PdCl_2$, 80 mg AA, 350 mg STAB, 5 mL ODE, and 5 mL OAM were mixed together in a 50 mL round-bottom flask. After keeping in a heating module at 80 °C for 1 hour, the flask was transferred into another heating module at 220 ℃ and kept at 220 ℃ for 2 hour under magnetic stirring. After the flask being cooled to room temperature, the products were collected and washed by centrifugation with a hexane/ethanol mixture for several times.

Ligand replacement reaction using the dopamine-based surfactant

α,ω-bis(2-carboxyethyl)polyethylene glycol (10 mg), NHS (3 mg), and dopamine hydrochloride (1.27 mg) were dissolved in pyridine (2 mL) that contained anhydrous sodium carbonate (1 mg). EDC (3 mg) was dissolved in $CHCl_3$ (100 μL) and added to the pyridine solution. At room temperature, the mixed solution was stirred for 3 hours before HEA nanoparticles (3 mg) was added, and the solution was shaken for overnight. The modified HEA nanoparticles were precipitated by adding hexane, collected by applying bar magnet and dried under vacuum for 1 hour. The product was then dissolved in PBS (3 mL, 137 mM NaCl, 2.7 mM KCl, 10 mM Na_2HPO4/KH_2PO_4, pH= 7.4). After a brief sonication, the dispersion was purified by filtering off the free surfactant though the Nanosep 100k OMEGA.

Synthesis of HOFs

1,4-benzenedicarboximidamide (2·2Cl, 0.78 mg), was dissolved in PBS (1 mL) to form solution A. Tetrakis(4-carboxylic acid phenyl) methane (TBA_4·4, 1.56 mg) was dispersed in H_2O (1 mL), followed by the addition of sodium hydroxide aqueous solution (2 M, 5 μL) to deprotonate TBA_4·4 (solution B). Thereafter, solution B was added to solution A under stirring conditions at room temperature. Precipitates were formed immediately upon mixing. The reaction mixture was left to gently stir for 5-10 min. The HOFs material was then recovered by centrifugation, and then washed, dispersed, and centrifuged three times in H_2O to remove any unreacted precursors.

Synthesize different HEAs (w/w %) ratios HEAs@HOFs (HH)

2·2Cl (0.78 mg), was dissolved in PBS (1 mL) to form solution A, followed by the addition of HEAs (0.3, 0.6, and 1.00 mg, respectively) and gentle magnetic stirring. TBA_4·4 (1.56 mg) was dispersed in H_2O (1 mL), followed by the addition of sodium hydroxide aqueous solution (2 M, 5 μL) to deprotonate TBA_4·4 (solution B). Thereafter, solution B was added to solution A under stirring conditions at room temperature. Precipitates were formed immediately upon mixing. The reaction mixture was left to gently stir for 5-10 min to obtain HEAs@HOF with different ratio of HEAs (10 wt%, 20 wt% and 30 wt%, respectively). The HOFs material was then recovered by centrifugation, and then washed, dispersed, and centrifuged three times in H_2O to remove any unreacted precursors.

Synthesize OMVs@HOFs (OH)

2·2Cl (0.78 mg), was dissolved in PBS (1 mL) to form solution A, followed by the addition of OMVs (100 μL) and gentle magnetic stirring. TBA_4·4 (1.56 mg) was dispersed in H_2O (1 mL), followed by the addition of sodium hydroxide aqueous solution (2 M, 5 μL) to deprotonate TBA_4·4 (solution B). Thereafter, solution B was added to solution A under stirring conditions at room temperature. Precipitates were formed immediately upon mixing. The reaction mixture was left to gently stir for 5-10 min to obtain OMVs@HOF. The HOFs material was

then recovered by centrifugation, and then washed, dispersed, and centrifuged three times in H_2O to remove any unreacted precursors.

Synthesis of OMVs@HEAs@HOFs (OHH)

2·2Cl (0.78 mg), was dissolved in PBS (1 mL) to form solution A, followed by the addition of HEAs (1.00 mg), OMVs (100 μL) and gentle magnetic stirring. TBA_4·4 (1.56 mg) was dispersed in H_2O (1 mL), followed by the addition of sodium hydroxide aqueous solution (2 M, 5 μL) to deprotonate TBA_4·4 (solution B). Thereafter, solution B was added to solution A under stirring conditions at room temperature. Precipitates were formed immediately upon mixing. The reaction mixture was left to gently stir for 5-10 min to obtain OMVs@HEAs@HOFs. The HOFs material was then recovered by centrifugation, and then washed, dispersed, and centrifuged three times in H_2O to remove any unreacted precursors.

Peroxidase-like Catalytic Activity Characterization.

The peroxidase-like activity of HEAs was evaluated *via* the catalytic oxidation of the TMB at the assist of H_2O_2. All the catalytic reactions were performed by monitoring the absorbance changes of TMB at 652 nm. In a typical test, chemicals were added into 960 μL HAc-NaAc buffer solution (10 mM, pH 4.0) in an order of 20 μL HEAs (final concentration 50 μg mL^{-1}), 10 μL TMB (final concentration 1 mM), and 10 μL H_2O_2 (final concentration 3 mM) under 37 °C, unless otherwise stated. The concentration, pH, T-dependent peroxidase-like activities were investigated by varying the concentrations of catalysts, TMB, H_2O_2, pH, and T.

Kinetic measurements.

Kinetic measurements were carried out in time course mode by monitoring the absorbance change of TMB at 625 nm. Experiments were carried out using 50 μg mL^{-1} HEAs, in a reaction volume of 1000 μL buffer solution (10 mM HAc-NaAc, pH 4.0, 37 °C) with 1 mM TMB as substrate, and different concentration of H_2O_2 concentration as substrate, and different concentration of TMB, unless otherwise stated. Accordingly, the oxidation rates of TMB by H_2O_2 were analyzed in terms of the Michaelis-Menten model: $\nu = V_{max}C/(K_m+C)$, where ν is the initial velocity, Vmax is the maximal reaction velocity, and C is the concentration of substrate. K_{cat} was calculated according to the equation: $K_{cat} = V_{max}/S$, where S is the concentration of catalyst.[1]

Photothermal performance of HEA NPs

HEA NPs solutions with different concentrations (50, 100, 200 μg mL^{-1}) were irradiated by 1064 nm laser at a power density of 1 W cm^{-2} for 600 s. The temperature was recorded every 20 s. To evaluate the photothermal conversion efficiency, HEA NPs solution (100 μg mL^{-1}, 1 mL) was heated to a steady temperature with a 1064 nm laser at a power density of 1 W cm^{-2} and then naturally cooled. The photothermal conversion efficiency was calculated according to the previous literature.[2]

$$\eta = \frac{hS(T_{max}-T_{surr})-Q_0}{I(1-10^{-A_{808}})} \quad (1)$$

$$\theta = \frac{T-T_{surr}}{T_{max}-T_{surr}} \quad (2)$$

$$t = -\tau_S ln\theta \quad (3)$$

$$\tau_S = \frac{m_d C_d}{hS} \quad (4)$$

$$Q_s = -\sum_i m_i C_{p,j} \frac{dT}{dt} = \frac{\sum_i m_i C_{p,j}(Tmax-Tsurr)}{t} \quad (5)$$

where η is the heat transfer coefficient, S is the surface area of container, T_{max} and T_{surr} are the maximum steady temperatures for HEA NPs solution and the ambient room temperature, Q_0 is the baseline energy input by the solvent and sample container without NPs, I is the incident laser power density, and A_{1064} is the absorbance of NPs solution at 1064 nm. The value of hS was calculated by Eq. (4), τs is the sample system time constant, m_d is the mass (g), C_d is the heat capacity [4.2×10^3 kJ/(kg·°C)] of water. The heat energy (Q_0) of the sample container and

solvent without HEA-Pd was measured independently using Eq. (3). The time constant was τ_s=236.5 s based on the linear fit from the cooling period after 600 s vs. -lnθ. Accordingly, the photothermal conversion efficiency calculated by Eq. (3) and Eq.(1) was η≈34.6%.

Cellular Uptake Behaviors of OHH

B16F10, 3T3 and RAW264.7 cells was randomly planted in 24-well plates and allowed to adhere for 24 h. After that, RB-PEG-SH modified OHH (100 μg mL^{-1}) was added and incubated with the cells. The cells were irradiated with1064nm laser for 5 minutes. After four hours, the cells were washed with PBS for 3 times, stained by Hoechst 33342 for 15 min before fluorescence analysis (images were obtained by using confocal laser scanning microscope).

In vitro Cytotoxicity Assay

MTT assay was used to determine the cytotoxicity of OHH nanoparticles. Briefly, B16F10, RAW264.7 and NIH3T3 cells were randomly seeded into 96-well plates at a density of 5000 cells per well (100 μL), respectively and were cultured at 37 °C with 5% CO_2 for 24 h. Different concentrations of OHH nanoparticles were added to the wells. The cells were subsequently incubated for 24 h in the CO_2 incubator. Then, 10 μL of MTT solution (5 mg mL^{-1}) was added to each well to a final volume of 100 μL. After that, the plate was placed in the CO_2 incubator for additional 4 h. The media was removed and DMSO (100 μL) was added into each well. Absorbance values were determined with Bio-Rad model-680 microplate reader at 490 nm (corrected for background absorbance at 630 nm). The cell viability was estimated according to the following equation: Cell viability (%) = ($OD_{Treated}$ /$OD_{Control}$) × 100%. Where $OD_{Control}$ was obtained in the absence of nanoparticles, and $OD_{Treated}$ was in the presence of nanoparticles.

Annexin V/PI Assay

B16F10 cells were randomly plated in 6-well plates and allowed to adhere for 24 h. Then the cells were incubated with OMVs，OH，HEAs and OHH (200 μg mL^{-1}). The cells in OHH group were irradiated with1064nm laser for 5 minutes. After 20 h, the cells were stained with 5 μL annexin V-FITC at room temperature for 15 min and followed by 10 μL PI for 5 min in the dark. The fluorescence intensity of cells was viewed by flow cytometry in green channel for annexin V-FITC and red channel for PI, respectively.

Live/Dead Assay

B16F10 cells were randomly plated in 6-well plates and allowed to adhere for 24 h. Then the cells were incubated with OMVs，OH，HEAs and OHH (200 μg mL^{-1}). The cells in OHH group were irradiated with1064nm laser for 5 minutes. The cells were incubated at CO_2 incubator for 18 h. Then fresh medium containing calcein-AM (5 μg mL^{-1}) and PI (10 μg mL^{-1}) was added. After cultured for 20 min, the cells were washed with PBS and imaged by an inverted fluorescence microscope.

Determination of ROS Generation in vitro

For ROS detection, B16F10 cells were randomly seeded in 6-well plates in DMEM for 24 h before further manipulation. Then cells were incubated with OMVs，OH，HEAs and OHH (200 μg mL^{-1}) for 8 h. The treated cells were washed with PBS twice and incubated with 10 μM of DCFH-DA for 30 min. After the unloaded probe was removed with PBS, the fluorescence intensity of cells was monitored by flow fluorescence microscopy.

Western blot-based analysis of tumor cell pyroptosis

B16F10 cells with a density of 10^5 cells per well were cultured in a 6-well plate for 24 h to allow the attachment of cells. Then the cells were incubated with OMVs，OH，HEAs and OHH (200 μg mL^{-1}) for 20h. After washing with PBS, the cells were digested with trypsin and collected into 1.5 ml tubes. They were blocked with 1% BSA and incubated with anti-γ-H2AX at room temperature for 1 h. The cells were incubated with Alexa Fluor 488-conjugated antibody for 30 min and analyzed by flow cytometry.

Western blot-based analysis of p-STING and p-IRF3

B16F10 cells with a density of 10^5 cells per well were cultured in a 6-well plate for 24 h to allow the attachment of cells. The cells were incubated with OMVs，OH，HEAs and OHH (200 μg mL^{-1}) for 24 h. After washing with PBS, the cells were collected into 1.5 ml tubes and resuspended in RIPA lysis buffer with protease inhibitor incubated for 10 min in an ice-bath and then centrifuged. The supernatant was collected, and BCA analysis was performed to determine the protein concentration. The protein samples were transferred to polyvinylidene fluoride membranes after electrophoresis and blocked with 5% BSA in TBST buffer at room temperature for 2 h. Then the membranes were incubated with primary antibodies in TBST buffer overnight at 4 ºC and rinsed in TBST buffer. The membranes were then incubated with a buffer solution containing horseradish peroxidase (HRP)-conjugated secondary antibodies at room temperature for 2 h and washed with TBST. Protein bands were tested by enhanced chemiluminescence detection.

Animal experiments

All animal procedures were performed in accordance with the Guidelines for Care and Use of Laboratory Animals of Changchun Institute of Applied Chemistry Chinese Academy of Sciences and approved by Institutional Animal Care and Use Committee of Changchun Institute of Applied Chemistry Chinese Academy of Sciences (Permit Number: 20210016). Healthy female Kunming mice (19-20 g) and female C57BL/6j mice (16-20 g) were purchased from the Laboratory Animal Center of Jilin University (Changchun, China). The tumor-bearing mouse model was established first in Balb/c mice. B16F10 cells (2×10^6 cells) were suspended in 100 μL of cell culture medium and subcutaneously injected into the back of mice.

In vivo systemic toxicity evaluation

To biocompatibility evaluation, Kunming mice were randomly divided into three groups (n=10), and intravenously injected with saline, OMVs and OHH (20 mg kg^{-1}, 100 μL). The mice's body weights were measured every 4 days to evaluate the in vivo biosafety. At the indicated time, the mice were euthanized and their blood samples were collected to perform a complete blood panel analysis
and serum biochemistry assay. Moreover, the major organs (heart, liver, spleen, lung, and kidneys) of mice were harvested for histological analysis.

Plasma pharmacokinetics

Rh B-modified OHH (OHH-RhB) (10 mg kg^{-1}) was intravenously administered to healthy Kunming mice. The major organs and tumors of the mice were collected at various time points post-injection, and imaged using the in vivo imaging system.

In vivo therapeutic evaluation:

B16F10 cancer bearing C57BL/6j mice were randomly divided into 5 groups (n=6). When the tumor volume reached about 100 mm^3, the mice were intratumorally injected with saline, OMVs, OH, HEAs and OHH (20 mg kg^{-1}, 100 μL), respectively. The tumor volume and body weight of mice were recorded every other day. The tumor volume was calculated as follows: $V = W^2 \times L/2$, where W and L represented the tumor width and length, respectively. The mice were sacrificed after 2 weeks post-treatment, and the tumors were collected and taken photos. The tumor growth inhibition (TGI) rate was calculated according to equation.

$$TGI = (1-V_T/V_C) \times 100\%$$

Where V_C represents the tumor volume of the control group, and V_T represents the tumor volume after the treatments.

Simultaneously, the major organs (heart, liver, spleen, lung, and kidney) and tumors of the mice were collected and used for histological and immunofluorescent staining.

Statistical analysis

In this article, all data were presented as mean result ± standard deviation (SD). All figures illustrated were obtained from several independent experiments with similar results. The statistical analysis was performed by using the Origin 2020 software.

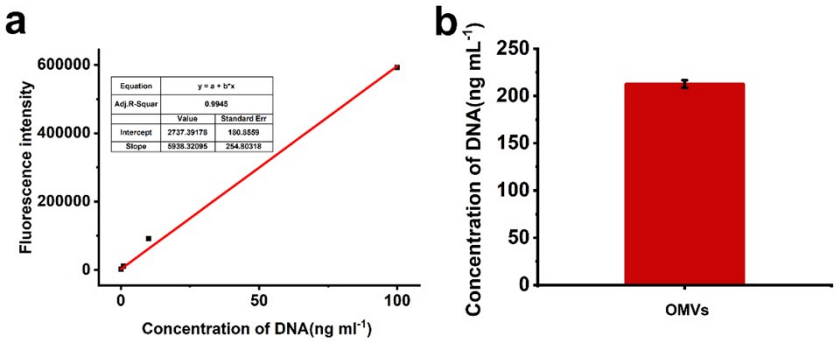

Figure S1. (a) Standard curve for determination of DNA concentration. (b) The concentration of DNA in the OMVs vesicles

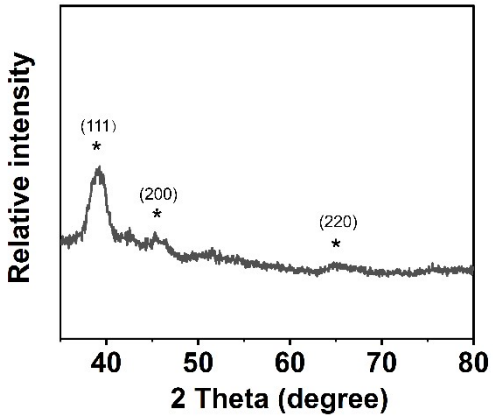

Figure S2. PXRD pattern of HEAs.

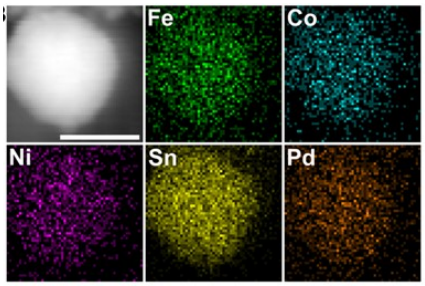

Figure S3. Dark-field TEM image and elemental maps of HEAs. Scale bar 50 nm.

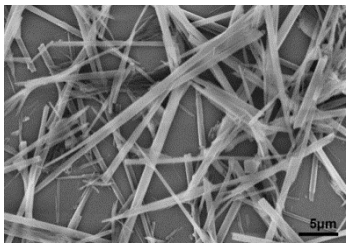

Figure S4. SEM image of HOFs.

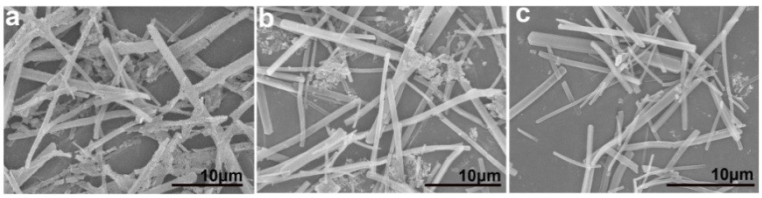

Figure S5. SEM image of HH with different amount of HEAs. (a) 10 wt % (b) 20 wt % (c) 30 wt %.

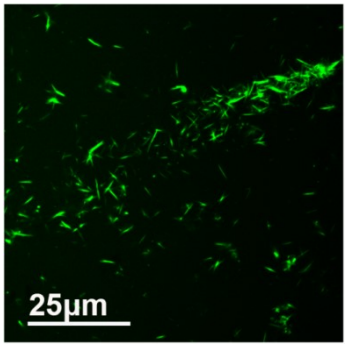

Figure S6. CLSM images of FITC-HEAs-HOFs.

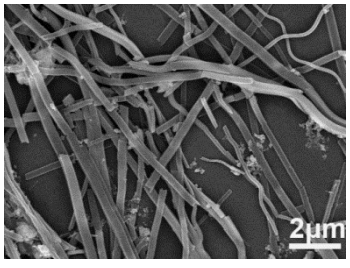

Figure S7. SEM image of OHH.

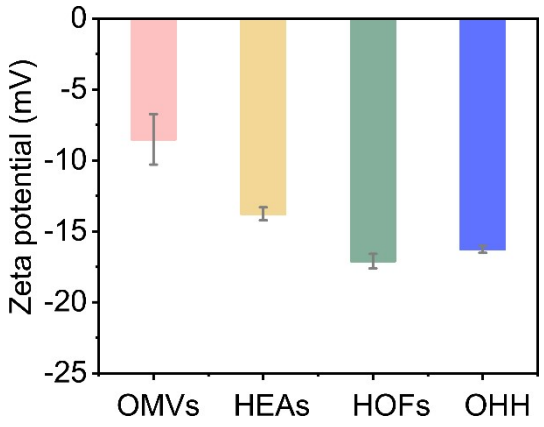

Figure S8. Zeta potentials of OMVs, HEAs, HOFs, and OHH NPs

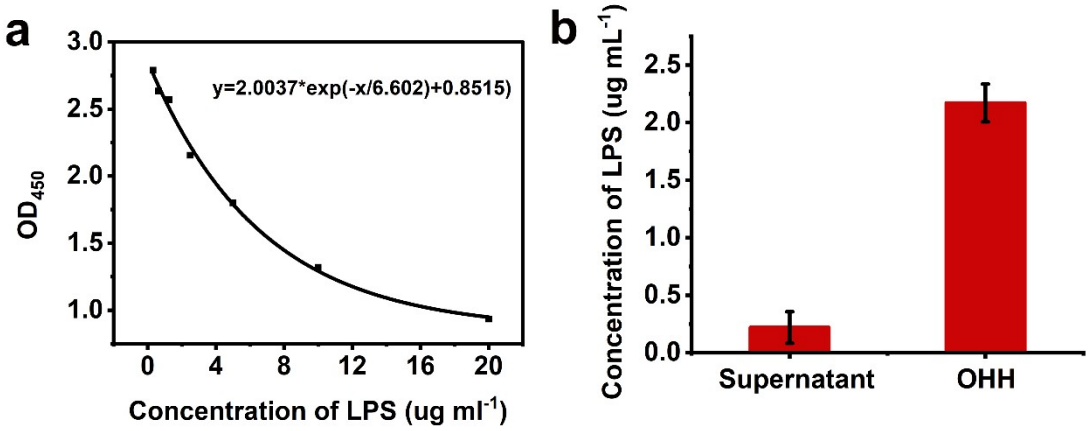

Figure S9. (a) Standard curve for determination of LPS concentration. (b) The concentration of LPS in the supernatant and OHH NPs after sonication.

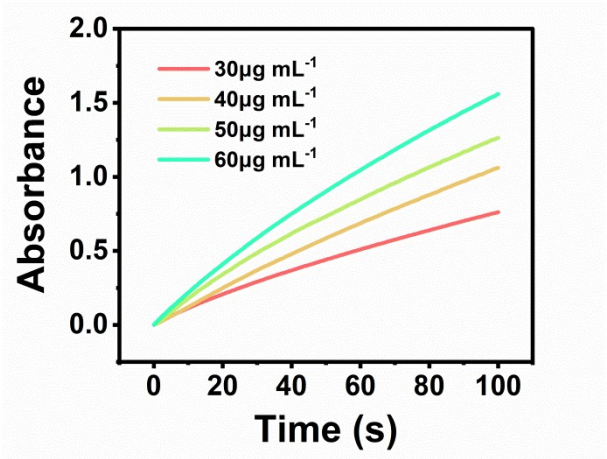

Figure S10. The absorbance of TMB solution treated with different concentrations of HEAs.

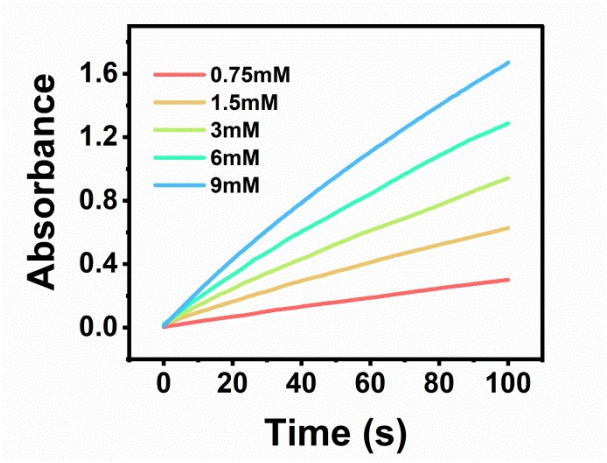

Figure S11. The time dependence of the absorbance with substrate H_2O_2.

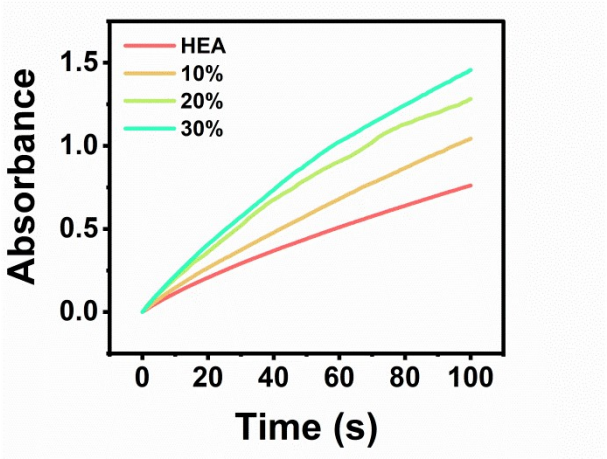

Figure S12. The absorption of TMB treated with OHH, containing different amounts of HEAs.

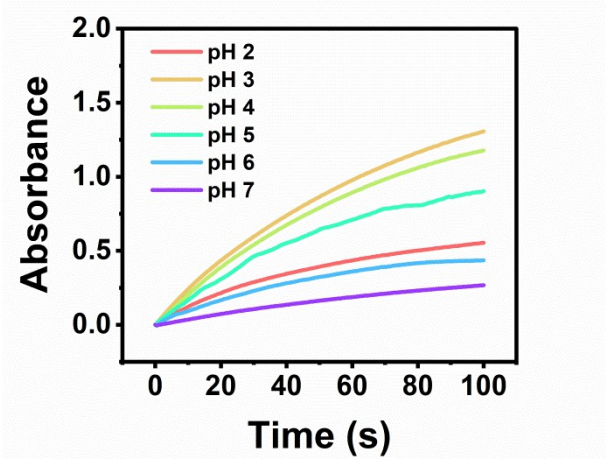

Figure S13. The absorption of TMB treated with OHH at different pH.

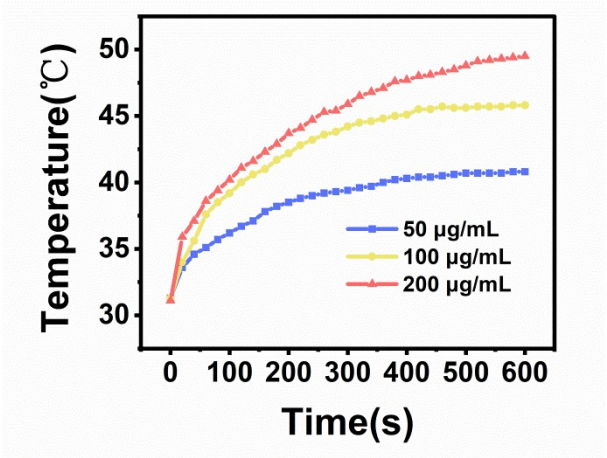

Figure S14. Photothermal-heating curves of HEAs dispersed aqueous suspensions at varied concentrations at 1 W·cm^{-2}

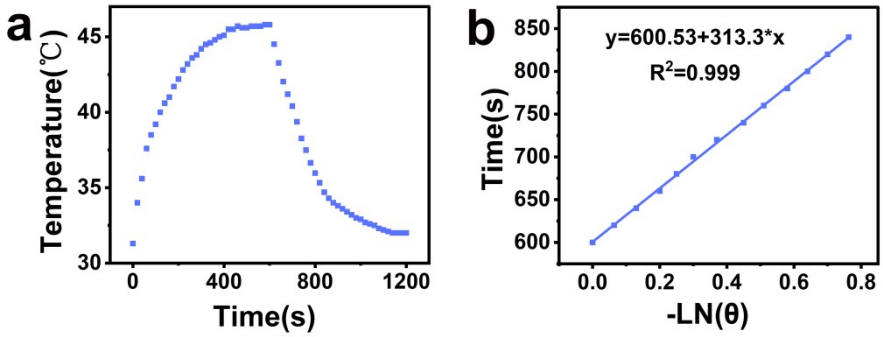

Figure S15. Calculation of the photothermal conversion efficiency of HEAs NPs.

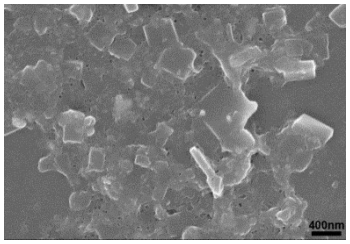

Figure S16. The disassembly of OHH observed by SEM.

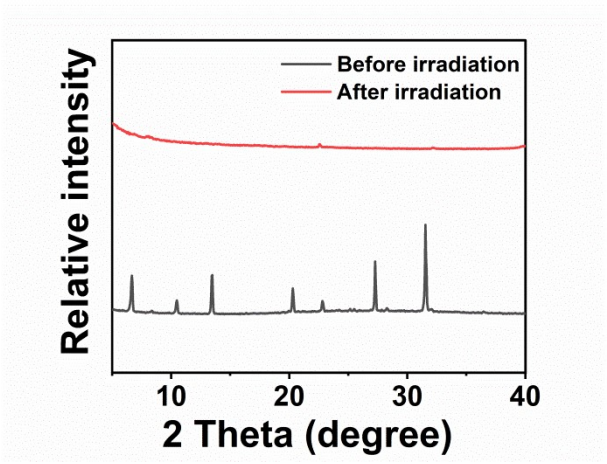

Figure S17. PXRD patterns of OHH (30 wt %) before and after irradiation.

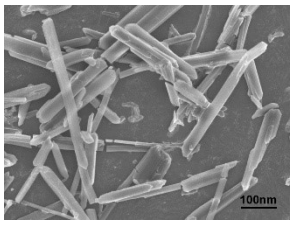

Figure S18. SEM images of OHH after treatment with the cell culture medium for 8 hours.

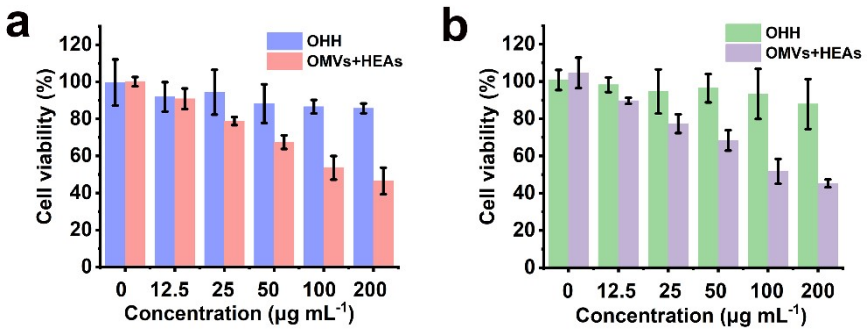

Figure S19. Viability of RAW264.7 cells (a) and NIH 3T3 cells (b) after 24 h treatment with OMVs and HEAs or OHH.

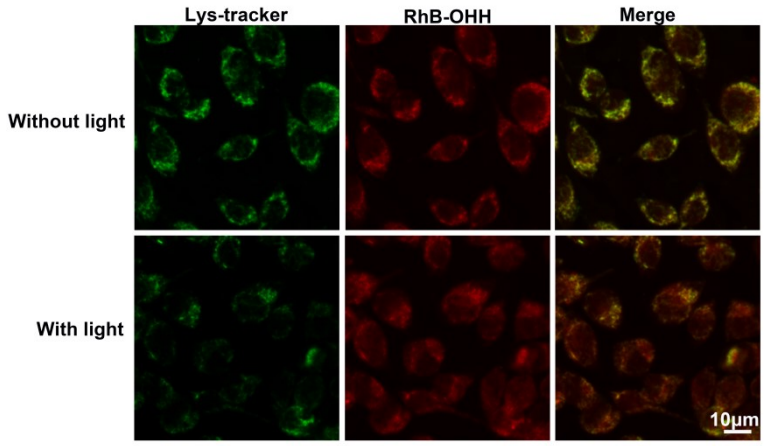

Figure S20. Fluorescence micrographs of cellular uptake against OHH with or without irradiation.

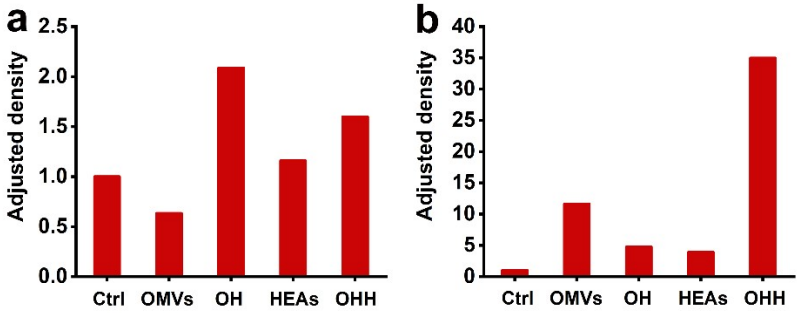

Figure S21. The adjusted density of the western blot images of p-STING (a) and p-IRF3 (b).

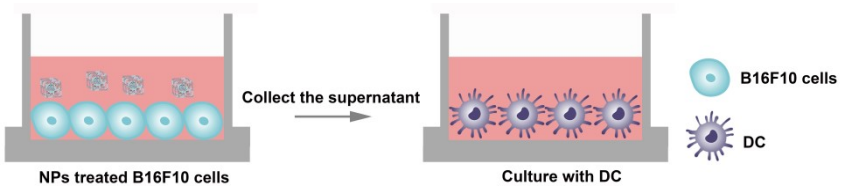

Figure S22. Scheme of activation of dendritic cell.

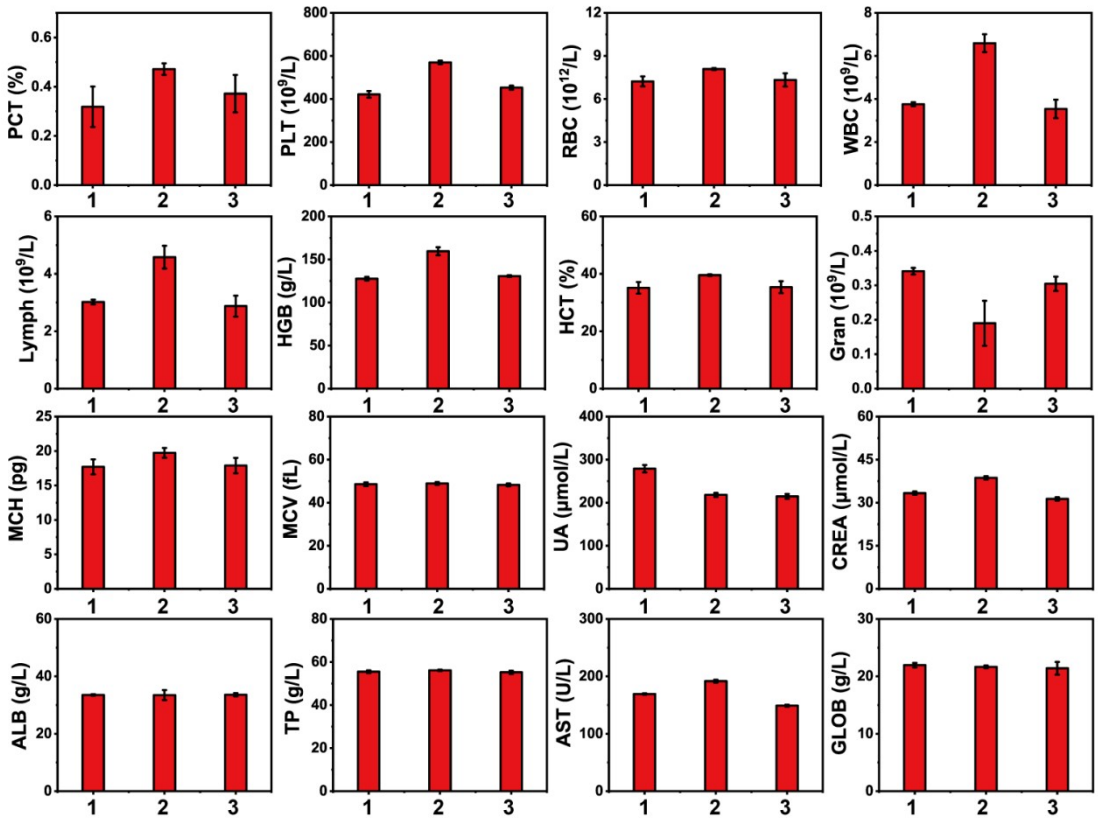

Figure S23. Biochemical and hematological analysis after 0 and 28 days post-injection (1: saline; 2: OMVs; 3: OHH).

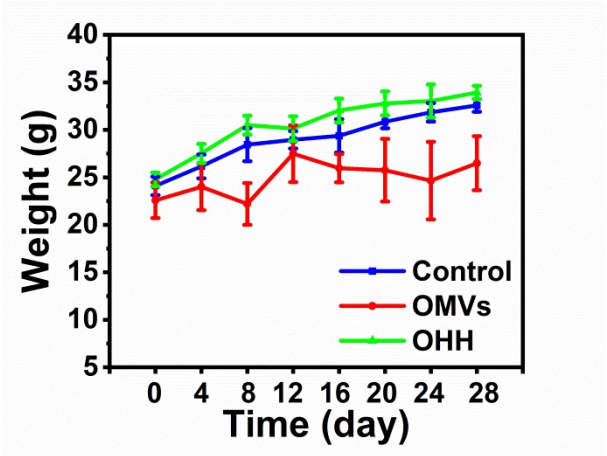

Figure S24. Body weights of mice treated with saline OMVs, and OHH while assessing the biocompatibility.

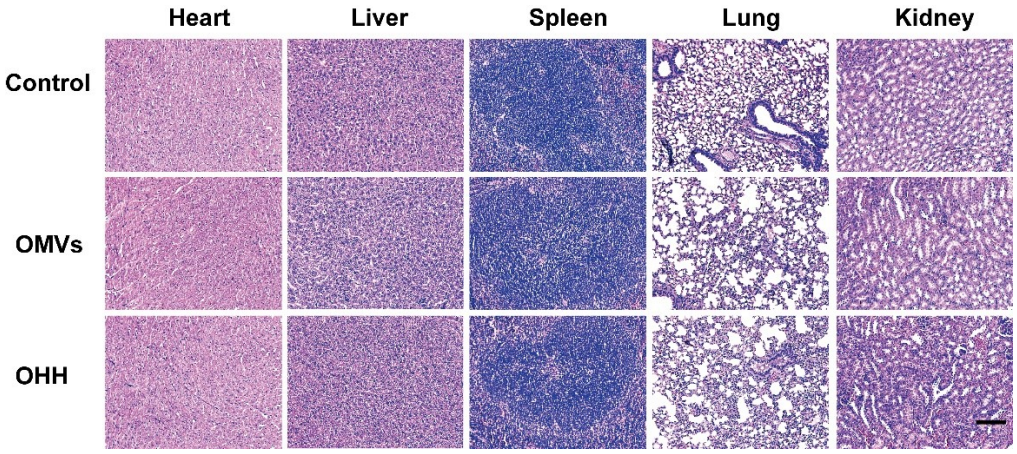

Figure S25. H&E staining images of histologic sections in the heart, liver, spleen, lung, and kidney after intravenously injecting saline OMVs, and OHH after 28 days. Scar bar 50 μm.

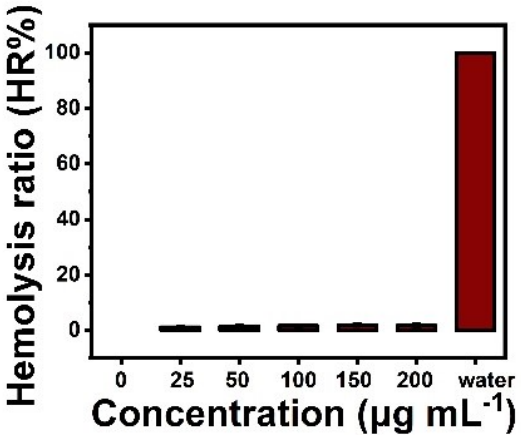

Figure S26. hemolysis rate of OHH nanoparticles.

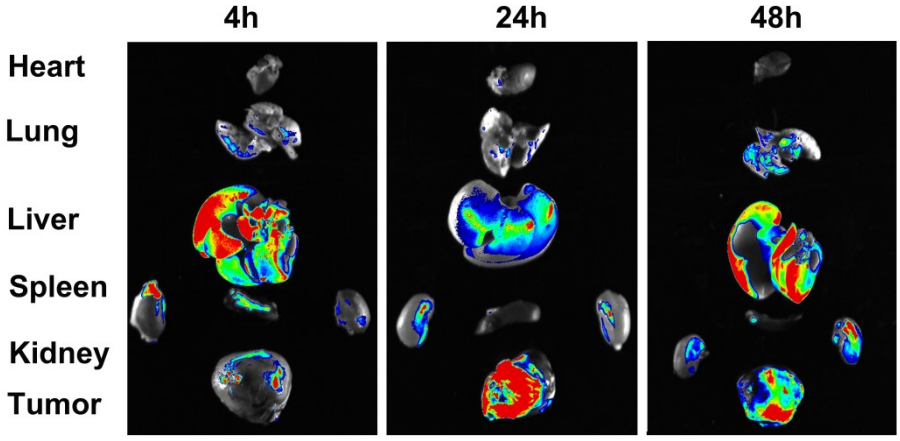

Figure S27. Distribution of RhB-OHH in different organs over time.

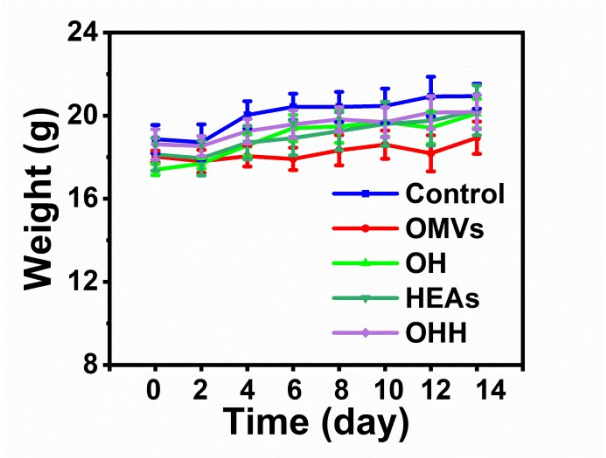

Figure S28. Body weights of mice after different treatments during antitumor therapy.

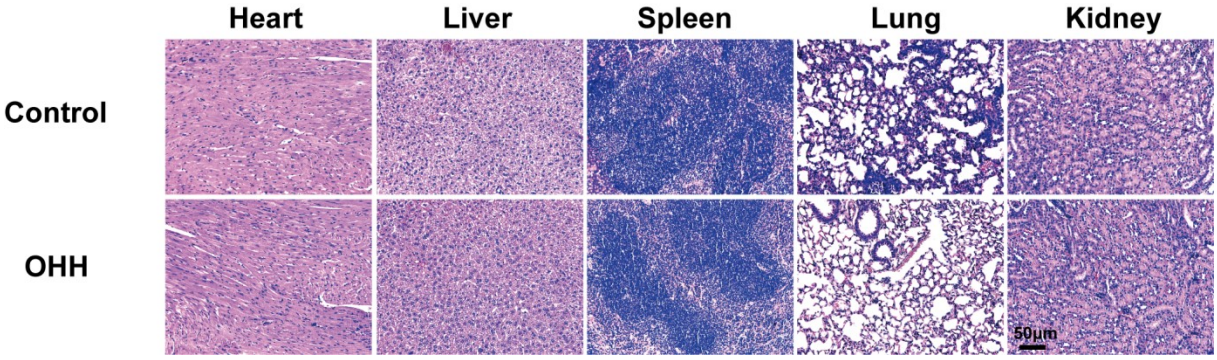

Figure S29. H&E staining images of histologic sections in the heart, liver, spleen, lung, and kidney of intravenously injecting saline and OHH after antitumor therapy.

References

[1] Y. Zhou, H. Sun, H. Xu, S. Matysiak, J. Ren, X. Qu, Angew. Chem. Int. Ed. 2018, 57, 16791-16795.

[2] L. Zhang, Y. Sang, Z. Liu, W. Wang, Z. Liu, Q. Deng, Y. You, J. Ren, X. Qu, *Angew. Chem. Int. Ed.* **2023**, *62*, e202218159.